LETTER

ACS chemical biology

High Affinity Binding to Profilin by a Covalently Constrained, Soluble Mimic of Phosphatidylinositol-4,5-bisphosphate Micelles

Sarah M. Richer[†], Nichole K. Stewart[†], Sarah A. Webb, John W. Tomaszewski, and Martha G. Oakley*

Department of Chemistry, Indiana University, 212 South Hawthorne Drive, Bloomington, Indiana 47405. [†]These authors contributed equally to this work.

ABSTRACT Phosphoinositide (PI) lipids are essential regulators of a wide variety of cellular functions. We present here the preparation of a multivalent analogue of a phosphatidylinositol-4,5-bisphosphate (PIP_2) micelle containing only the polar headgroup portion of this lipid. We show that this dendrimer binds to the cytoskeletal protein profilin with an affinity indistinguishable from that of PIP_2, despite the fact that profilin discriminates between PIP_2 and its monomeric hydrolysis product inositol-1,4,5-triphosphate (IP_3) under physiological conditions. These data demonstrate that the diacylglycerol (DAG) moiety of PIP_2 is not required for high-affinity binding and suggest that profilin uses multivalency as a key means to distinguish between the intact lipid and IP_3. The class of soluble membrane analogues described here is likely to have broad applicability in the study of protein·PI interactions.

Phosphoinositide (PI) lipids play important roles in virtually every cellular process in eukaryotes, including cell motility and the regulation of the cytoskeleton, membrane trafficking, apoptosis, and cell growth (*1–6*). These lipids are recognized by a variety of structurally distinct protein domains, including PH, PX, FERM, ANTH, ENTH, and Tubby domains (*7–11*), as well as by proteins containing surface patches of basic residues (*12–17*). Our understanding of the role of protein·PI interactions and the regulation of protein function by PIs has advanced significantly in the past decade (*2*). However, the study of the molecular basis for these interactions has been hampered by the inherent complexity of eukaryotic cell membranes, by the mobility of lipids within the bilayer, and often by the requirement for interactions with multiple membrane components (*2, 7, 18*).

Indeed, many PI-binding proteins form multivalent complexes with their lipid targets (*9, 11–16, 19–23*). The importance of multivalent interactions for the recognition of biological molecules is especially well documented for carbohydrate-binding proteins, and synthetic multivalent ligands capable of displaying multiple copies of mono- and oligosaccharides have been vital for studying these interactions (*24–26*). Similarly, synthetic analogues of lipid assemblies would provide an extremely valuable tool for probing and manipulating protein·PI interactions.

Many PI-binding proteins are peripheral membrane proteins that are likely to interact primarily with polar lipid headgroups (*2, 4, 10*). We therefore reasoned that a multivalent PI analogue lacking the hydrophobic diacylglycerol (DAG) moiety would be an effective ligand, greatly simplifying the preparation of these analogues. Human profilin I, a tumor suppressor (*27–29*) that is involved in the regulation of the cytoskeleton (*30, 31*), was used for our initial studies. This small, well-characterized, actin-binding protein also recognizes phosphatidylinositol-4,5-bisphosphate (PIP_2), interacting with multiple equivalents of lipid (*12, 13, 32–36*). Importantly, profilin can discriminate between PIP_2 and its monomeric hydrolysis product, inositol-1,4,5-triphosphate (IP_3), and this discrimination appears to be important for its function (*37*). We chose polyamidoamine (PAMAM) dendrimers as our polymeric scaffold because of their aqueous solubility, extensive structural characterization, and commercial availability (*38*). Moreover, the larger branched polymers in this class adopt a spherical shape, providing a micelle-like arrangement of lipid headgroups (*39*).

Here, we present the synthesis of a PAMAM dendrimer derivatized with 46 PIP_2 headgroups. Moreover, we show that this

***Corresponding author, oakley@indiana.edu.**

Received for review May 27, 2009 and accepted July 10, 2009.

Published online July 13, 2009

10.1021/cb900121r CCC: $40.75

Scheme 1. General Scheme for the Synthesis of G4 PAMAM PIP_2 Dendrimer 1[a]

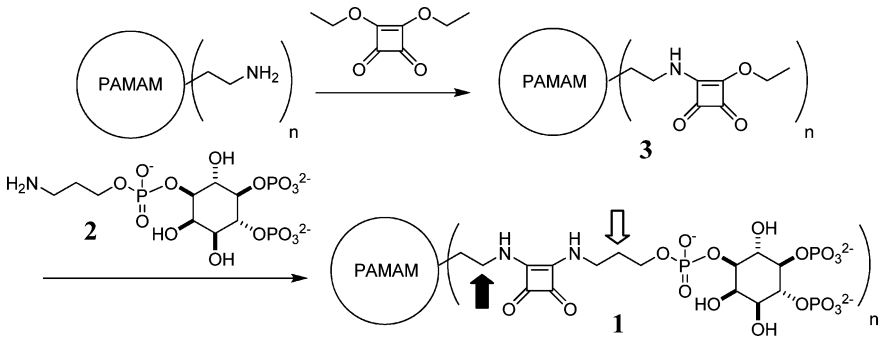

[a]Arrows correspond to those shown in Figure 1.

artificial micelle binds to profilin with an affinity equivalent to that of PIP_2. This result demonstrates that micelle mimics containing only the headgroup portion of a PI lipid can bind with high affinity even to a protein that discriminates between PIP_2 and IP_3.

We have previously described the attachment of an aminoalkyl-tethered PIP_2 headgroup analogue **2** (*40–42*) to generation 0 (G0) and generation 1 (G1) PAMAM dendrimers *via* a 3,4-diethoxy-3-cyclobutene-1,2-dione (squarate) linker (*43*). For this study, the generation 4 (G4) PAMAM dendrimer was selected as the most suitable scaffold, as its size and the number of termini available for attachment of PIP_2 headgroups (*38, 39*) would afford a modified dendrimer with roughly the size and headgroup spacing of a PIP_2 micelle (*44*). Unlike the smaller PAMAM dendrimers, the G4 dendrimer is polydisperse as a result of defects in polymer synthesis (*45*). We found the G4 PAMAM dendrimer to have 60 available termini, in accord with previously reported values (*45–47*). The dendrimer was derivatized with diethyl squarate (*48*) to afford G4 PAMAM squarate dendrimer **3** (Scheme 1). Approximately 51 termini were modified as judged by matrix-assisted laser desorption/ionization-time-of-flight (MALDI-TOF) mass spectrometry.

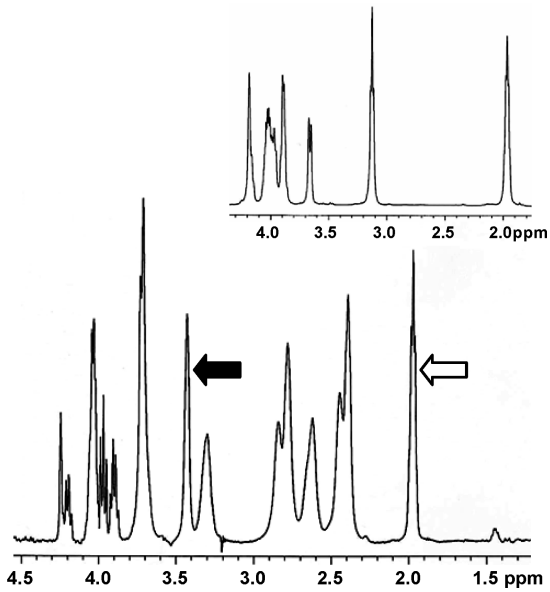

Figure 1. ^{1}H NMR spectra for G4 PAMAM PIP_2 dendrimer 1 and PIP_2 headgroup 2 (inset). The well-resolved peaks used to determine the number of headgroup moieties coupled to the dendrimer are indicated by open and filled arrows, respectively.

PIP_2 aminoalkyl headgroup **2** was coupled to squarate dendrimer **3** to afford G4 PAMAM PIP_2 dendrimer **1**. The progress of the reaction was monitored by ^{1}H NMR, through the disappearance of the squarate ethyl resonance at 1.46 ppm (OCH_2CH_3) (Figure 1). The degree of derivatization of the product dendrimer was estimated using ^{1}H NMR, by comparison of relative integrals located at well-defined resonances (Figure 1, open and closed arrows). Approximately 90% of the squarate-containing termini were derivatized, affording dendrimer **1** with an average of 46 PIP_2 headgroups per dendrimer.

To assess the suitability of artificial micelle **1** for studying protein·PI interactions, we monitored its binding to profilin, which binds to both PIP_2 micelles and large unilamellar vesicles (LUVs) containing PIP_2 (*12, 13, 32–36*). Biochemical studies with profilin are complicated by its sensitivity to modifications at either terminus (*34, 49, 50*), requiring the use of unlabeled protein. We therefore measured the binding affinity of profilin for PIP_2 and for G4 PAMAM PIP_2 dendrimer **1** using an enzyme-linked immunosorbent assay (ELISA). ELISA plates were coated with PIP_2 or dendrimer **1** and then incubated with varying amounts of profilin. The bound profilin was affixed with a primary antiprofilin antibody, which was in turn detected by means of a secondary horseradish peroxidase (HRP)-conjugated antibody. The data were fit assuming a 1:1 binding model, yielding an average dissociation constant (K_d) of 6.5 $\pm$ 4.9 μM for the profilin·PIP_2 interaction (Figure 2, panel a), consistent with previously reported values (*13, 32–36*). The affinity of profilin for G4 PAMAM PIP_2 dendrimer **1** is indistinguishable from that of PIP_2, with a K_d of 4.6 $\pm$ 4.5 μM (Figure 2, panel a). Independent controls confirmed that there was no interaction between profilin and an unmodified dendrimer lacking the PIP_2 headgroup **2** (data not shown).

To characterize the complex between profilin and dendrimer **1** further, we sought to estimate the average number of profilin molecules bound to each dendrimer using sedimentation equilibrium experiments. Be-

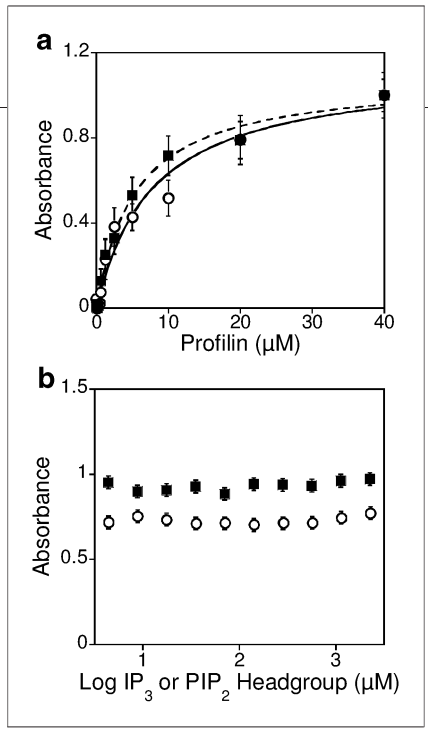

Figure 2. ELISA binding data for profilin. a) Average normalized fitted ELISA data for binding titrations of profilin with PIP_2 (circles, solid line) and G4 PAMAM PIP_2 micelle mimic 1 (squares, dashed line). The dissociation constants reported were derived from 15 separate experiments for both PIP_2 and 1; error bars represent the standard deviation of these experiments. b) Representative data from competition titration experiments for IP_3 (circles) and PIP_2 headgroup 2 (squares). Neither ligand was able to compete with PIP_2 (0.2 μM) for binding to profilin (10 μM) even at a >20,000-fold excess. Error bars represent the standard deviation of the profilin signal in the absence of either ligand from 88 wells.

cause of the polydispersity of the dendrimer pool and the potential for multiple profilin molecules to interact with each dendrimer, we expected a distribution of complexes. To minimize this heterogeneity, we used a 13-fold excess of profilin and monitored the complex at a wavelength (305 nm) at which the absorbance is due primarily to the dendrimer squarate moiety. Data were fit to an idealized single-species model to obtain an average molecular weight for the distribution of species. The observed molecular weight of ca. 170 ± 17 kDa mol^{-1} corresponds to that expected for a single dendrimer bound to 8 ± 1 molecules of profilin, providing a binding stoichiometry of approximately 1 profilin per 6 PIP_2 headgroups (data not shown). Estimates of the stoichiometry of the profilin·PIP_2 interaction range from 5−10 molecules of lipid per molecule of profilin (*12, 13, 32–35*). In general, higher estimates are obtained with PIP_2 micelles than with PIP_2-containing LUVs, presumably because there is insufficient surface area on the micelles to accommodate additional protein molecules. Similarly, steric occlusion may also limit the number of profilin molecules that interact with each dendrimer; thus, we interpret the 1:6 stoichiometry we observe for the dendrimer as an upper limit. Nonetheless, these data are consistent with the profilin·PIP_2 binding stoichiometry values reported in the literature (*12, 13, 32–35*), emphasizing the importance of multivalency for the interaction between profilin and dendrimer **1** and indicating a binding mode similar to that observed for PIP_2.

To assess the efficacy of G4 PAMAM PIP_2 dendrimer **1**, it is necessary to measure not only the binding affinity of profilin for PIP_2 but also its affinity for monomeric IP_3. Although a profilin·IP_3 complex has not been detected at physiological concentrations in a wide variety of biochemical assays (*32, 33, 51, 52*), we have recently shown that profilin binds to IP_3 at elevated concentrations. Using $^1H-^{15}N$ HSQC NMR titrations, we determined an average apparent K_d value of 20 mM for the profilin·IP_3 (*53*). For direct comparison to our PIP_2 and G4 PAMAM PIP_2 dendrimer **1** ELISA data, we probed the ability of profilin to bind PIP_2 in the presence of excess IP_3 or PIP_2 headgroup **2** using competition ELISA (Figure 2, panel b). No change in the affinity of profilin for PIP_2 was detected in the presence of either ligand in excess of 20,000 equiv (Figure 2, panel b). We therefore estimate from these results a lower limit of 10 mM for the dissociation constants of these complexes, in accord with our previously reported NMR results (*53*). Thus, profilin binds to its target lipid, PIP_2, with approximately 3000-fold higher affinity than it does to IP_3. Moreover, all of this binding affinity is recovered in the multivalent ligand, G4 PAMAM PIP_2 dendrimer **1**, which does not contain the DAG moiety. This result is particularly remarkable as the spacing between headgroups of our analogue has not been optimized.

Our observation of high-affinity binding to profilin by a multivalent PI analogue completely lacking the DAG moiety strongly suggests that this hydrophobic portion of the lipid is not required for binding. In contrast, multiple PIP_2 headgroups are required for high-affinity binding. The simplest interpretation of these observations is that the acyl chains are required for lipid self-association, allowing multivalent presentation of PIP_2 headgroups within the membrane (Figure 3). Supporting this view, Moens *et al.* (*54*) have shown that PIP_2 at submicellar concentrations has a dramatically lower binding affinity for profilin than does PIP_2 in micelles or lipid vesicles. The observed K_d (1 mM) for the interaction between profilin and submicellar PIP_2 is approximately 20-fold lower than the K_d we have reported for

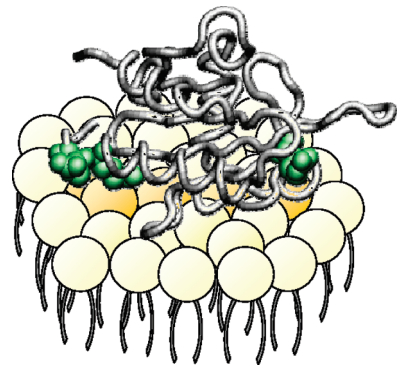

Figure 3. Schematic representation of the multivalent interaction between profilin and PIP_2. Profilin (gray) is shown binding to a membrane (yellow) with PIP_2 headgroups shown in orange. Residues implicated in binding are shown in green. The protein model was prepared in Visual Molecular Dynamics (University of Illinois and the Beckman Institute) using 1FIK (*72*).

the profilin·IP_3 interaction (*53*). Because our data demonstrate that the DAG moiety is not required, the increased affinity of profilin for "monomeric" PIP_2 relative to IP_3 may indicate self-association of the acyl chains on the surface of profilin. Indeed, profilin has been observed to cluster PIP_2 molecules in model membranes (*54*).

A subset of PI-binding domains, most notably PH domains, interact strongly with both lipid bilayers and monovalent headgroups (*55*) and can be studied using soluble, monovalent PI probes. Indeed, such probes have been critical tools for identifying PI-binding proteins and for investigating their mechanism of action *in vitro* and *in vivo* (for a review, see ref 56). However, our work suggests that multivalent probes are required for recognition of proteins that bind weakly to individual PI headgroups but bind strongly to lipid assemblies.

Profilin is only one example of a number of PI-binding proteins for which multivalent interactions are important. Well-characterized proteins that bind to multiple PI ligands include gelsolin (*14, 16*), N-WASP (*21*), and FERM domain proteins (*3*). In addition, proteins such as myosin X, dynamin, and some FYVE domain proteins contain multiple lipid-binding domains or require dimerization for productive membrane binding (*9, 11, 22, 23*). Multivalent analogues, such as the dendrimers described here, the cross-linked PI liposomes developed by Prestwich and co-workers (*57*), or the surface display of synthetic PI headgroups described by Best and co-workers (*58*) would be expected to bind to all of these proteins with substantially greater affinity than would monovalent PI ligands.

The use of covalently constrained, multivalent PI analogues also provides key advantages over lipid micelles and vesicles. First, covalently constrained micelle analogues can be used at concentrations below the critical micelle concentration (*54*). Second, the methods we describe here can be adapted to prepare PI probes containing different headgroups (*40, 59*). These synthetic analogues would allow for the study of the protein−lipid specificity without the changes in lipid aggregation properties that accompany changes in phosphorylation state and complicate the analysis of protein·PI interactions (*60, 61*). Third, the average spacing between PI headgroups can be readily varied to probe the determinants of binding specificity for different classes of PI-binding proteins (*62–64*). Fourth, similar strategies allow the preparation of co-polymers presenting additional lipid or protein determinants of specificity. Finally, our multivalent PI analogues have potential applications not only for biochemical assays but also for the study of PI-binding proteins in cell culture.

In conclusion, we have demonstrated that a PI-containing dendrimer lacking a hydrophobic moiety binds profilin with an affinity indistinguishable from that of PIP_2, even though profilin fails to bind to monovalent headgroups at physiologically relevant concentrations. This result sets the stage for the preparation of a new class of covalently constrained, multivalent PI probes, a powerful new tool for the characterization of PI·protein interactions.

METHODS

The plasmid pMW172 was a kind gift from S. C. Almo. Chemicals were obtained from Sigma Aldrich unless otherwise noted. Dendrimers were obtained from Dendritech. Dialyses were carried out using either Spectra/Por R6 dialysis membranes (Spectrum Laboratories, Inc.) or Tube-O-Dialyzers (G-Biosciences/Genotech). The latter apparatus was found to lead to better recovery. NMR spectra were collected using either a 400 (^{1}H) or 500 (^{1}H) MHz Varian Inova NMR spectrometer. Samples were externally referenced to H_3PO_4 (85%) for ^{31}P NMR spectra or DSS (sodium 2,2-dimethyl-2-silapentane-5-sulfonate) for ^{1}H and ^{13}C NMR. ^{1}H and ^{31}P NMR data were analyzed using MestReC (Mestrelab Research S.L.). Mass spectra were acquired using MALDI-TOF (Bruker Biflex III MALDI-TOF mass spectrometer with reflectron).

Protein Expression and Purification. Human profilin I was expressed using the T7 bacteriophage expression system (*65*). The pMW172 construct was transformed into the *E. coli* strain BL21(DE3) (Novagen) and purified essentially as described by Fedorov *et al.* (*65*), without the use of an anion exchange column. In addition, we found that substitution of β-mercaptoethanol (βME) for dithiothreitol minimized protein precipitation and methionine oxidation. Therefore, βME (1 mM) was used in all buffers. The mass of purified profilin is consistent with that expected for the protein after complete removal of the amino terminal methionine residue. MALDI-TOF: calcd for $C_{657}H_{1046}N_{180}O_{202}S_7$ 14,923.0; obsd $[M + H]^+$ 14,923.6.

ELISA Assays. Binding of profilin to PIP_2 or G4 PAMAM PIP_2 dendrimer **1** was investigated by ELISA. Greiner medium bind polystyrene plates (Sigma Aldrich) were coated overnight at 4 °C with 10 or 25 pmol per well of 1:5 PIP_2/PC in 1:9 $CHCl_3$/MeOH (*66*) or G4 PAMAM PIP_2 dendrimer **1** in 0.1 M $NaHCO_3$ pH 9. As a control, 10 or 25 pmol per well of bovine serum albumin (BSA) was coated in 0.1 M $NaHCO_3$ using the same conditions as described above. After removal of excess liquid, the plates were washed with phosphate buffered saline with Tween (PBST; 140 mM NaCl, 5 mM sodium phosphate, 0.02 % Tween, pH 7.4) and blocked with 3% BSA in PBS (140 mM NaCl, 5 mM sodium phosphate, pH 7.4) for 1 h at RT. After the PBST washes, the plates were incubated with increasing profilin (up to 2000 pmol in 10 mM Tris-Cl, 40 mM KCl, 1 mM βME, pH 8) for 2 h at RT. Free profilin was removed by washing with PBST, and bound profilin was incubated for 1 h at RT using a specific antiprofilin rabbit antibody (Gene Tex, Inc.; diluted 1:5120 in PBS). Unbound antibody was removed by washing with PBST followed by incubation for 1 h at RT with a secondary goat antirabbit HRP-conjugated antibody (Gene Tex, Inc.; diluted 1:1000 in PBS). Following PBST washes, secondary HRP-conjugated antibody was detected using 3,3′,5,5′-tetramethylbenzidine (Invitrogen). The reaction was quenched using 1 N HCl, and the absorbance was quantitated at 450 nm. In all trials, the binding volume was 50 μL, and in all washing steps the plates were washed up to 5 times with PBST.

For the competition ELISA experiments, all steps were carried out as described above except only 10 pmol of PIP_2 was used per well and the profilin incubation step was altered. Profilin, 10 μM, was preincubated with IP_3 or **2** (up to 209,000 pmol) for 20 min at RT before applying the mixture to the ELISA plates. Four and six independent data sets were obtained for compound **2** and for IP_3, respectively, all of which reproduce the results shown in Figure 2, panel b. A lower limit for the K_d was estimated by calculating the lowest K_d for which no change would be observed outside of the calculated error in the profilin·PIP_2 complex (*67*).

Since the degree of cooperativity has not been unambiguously determined for binding of profilin to PIP_2 or to the G4 PAMAM PIP_2 dendrimer **1**, all data were fit to a 1:1 binding model using Kaleidagraph 4.03 (Synergy Software) as described by Ye *et al.* (*68*). Data from each titration were normalized to account for variability in absorbance.

Because nonspecific binding of profilin to the plates was significant, each titration involving profilin was repeated using BSA-coated wells to control for background binding. Only data sets in which the maximum absorbance value in the pres-

ence of PIP_2 or dendrimer **1** was at least twice that observed in their absence were included in the reported affinity constants (ca. 70%). Absorbance values were corrected for background before the data were fit (Supplementary Figure 1). The error for the K_d measurements was determined using the standard deviation between the K_d values of individual ELISA plates.

Sedimentation Equilibrium. Apparent molecular masses were determined by sedimentation equilibrium with a Beckman XL-I ultracentrifuge at 20 °C. The concentrations of the G4 PAMAM PIP_2 dendrimer **1** and profilin were 23.6 and 315 μM, respectively (in 10 mM Tris-Cl, 40 mM KCl, 1 mM βME, pH 8). Data were obtained at 305 nm, a wavelength at which the observed absorbance is primarily due to the squarate moiety, for three rotor speeds (6,000, 7,500, and 9,000 rpm) using an An-60Ti rotor (Beckman). Data were fit simultaneously to a single species model of absorbance versus radial distance using the Origin (XL-A/XL-I data analysis software version 4.0, Beckman Instruments, Inc.) software provided by the manufacturer. The solvent density and the partial specific volume of profilin were calculated using SEDNTERP (*69*). A partial specific volume of 0.790 mL g^{-1} was used for the derivatized G4 dendrimer (*70*).

G4 PAMAM Squarate Dendrimer (3). The number of free amines in the G4 PAMAM dendrimer starting material was determined by subtraction of the observed MW of 13,783 g mol^{-1} by MALDI-TOF from the theoretical MW and division by 114 g mol^{-1} (equivalent to the mass of one terminal $-CH_2CH_2CONHCH_2CH_2NH_2$) (*45*). Polydispersities were calculated according to Woller and Cloninger (*46*).

G4 PAMAM dendrimer containing an average of 60 free amine termini was concentrated from a methanolic solution (100 mg, 7.19×10^{-3} mmol) in a glass vial. The dendrimer was then dissolved in DMSO (2 mL), and 3,4-diethoxy-3-cyclobutene-1,2-dione (diethyl squarate) (59 μL, 68 mg, 0.401 mmol) was added. The reaction mixture was stirred at ambient temperature overnight. Residual diethyl squarate was removed by dialysis against DMSO (2×1000 mL, 1000 MWCO cellulose tubing).

The extent of reaction was determined by subtraction of the observed MW by MALDI-TOF from the observed MW of the G4 PAMAM dendrimer and division by 125 (equivalent to the mass of one terminal squarate moiety; see Scheme 1). The polydispersity index increased slightly upon modification, as has been observed for glycosylated PAMAM dendrimers (*46*). For the polymer used in this experiment, approximately 85% of the termini were modified by squarate. Subsequent experiments demonstrated that yields of up to 92% could be obtained by the addition of a slight excess (1.05) of diethyl squarate per free amine. Isolated yield: 77 mg, 3.9×10^{-3} mmol, 51%. ^{1}H NMR (400 MHz, DMSO-d_6) δ: 8.68 (1 H, br s, N*H*), 8.51 (1 H, br s, N*H*), 7.98 (br s, N*H*), 7.72 (br s, N*H*), 4.62−4.56 (2 H, qrt, $-OCH_2CH_3$), 3.45 (br s), 3.17 (br s), 3.03 (br s), 2.54 (br s), 2.40 (br s), 2.19 (br s), 1.46 (3 H, tr, $-OCH_2CH_3$). ^{13}C NMR (125 MHz, DMSO-d_6) δ: 189.1, 182.3, 182.1, 176.9, 176.4, 172.9, 172.5, 171.6, 171.2, 68.8, 52.1, 49.4, 43.7, 43.3, 36.8, 33.1, 15.6 (Supplementary Figure 2). IR (ATR) cm^{-1}: 3268, 3206, 3073, 2968, 2937, 2829, 1801, 1700, 1649, 1603, 1544, 1482, 1431, 1377, 1334, 1256, 1023, 949. MALDI-MS: calcd for 13,783 + (51 × 170) − (51 × 46) 20,083; found 20,082.

G4 PIP_2 Dendrimer (1). The amine-tethered PIP_2 lipid headgroup analogue **2** was prepared as described previously (*41–43, 71*). Absolute ethanol (225 μL) and 0.1 M $NaHCO_3$ buffer, pH 9 (225 μL) were added to the G4 PAMAM squarate dendrimer **3** (15 mg, 7.47×10^{-4} mmol of **3** based on MW of 20,082 as determined by MALDI-TOF) and aminoalkyl headgroup **2** (47.5 mg, 8.09×10^{-2} mmol) in a 1.5-mL Eppendorf tube. The mixture formed a cloudy suspension and was allowed to stir at ambient temperature for 48 h. Ethanol was then removed *in vacuo* to give a clear yellow solution. The reaction was monitored by ^{1}H NMR (H_2O/D_2O) over 30 days, and the extent of the reaction was determined by the disappearance of the ^{1}H resonance at δ 1.46 (m, $-OCH_2CH_3$), corresponding to the remaining squarate ethyl group from unreacted **3**. Excess headgroup **2** was removed by extensive dialysis against 0.1 M $NaHCO_3$ buffer, pH 9 (1000 MWCO).

The degree of derivatization (90%) of the G4 PAMAM squarate dendrimer with PIP_2 aminoalkyl headgroup **2** was determined by ^{1}H NMR, using the relative integrals for the terminal methylene of the PAMAM dendrimer core (δ 3.45, R-$NHCH_2CH_2$-) and the middle methylene of the PIP_2 headgroup aminoalkyl tether linker (δ 1.98, R-$OCH_2CH_2CH_2NH$-) (see Figure 1, closed and open arrows, respectively). To allow for complete ^{1}H relaxation between scans, T_1 values for all protons in the G4 PAMAM PIP_2 dendrimer **1** were measured. T_1 values for the protons used to calculate the degree of derivitization (Figure 1) ranged from 0.41 to 0.65 s. Thus, a recycle delay of 5 s ($>5 \times T_1$) was used for all ^{1}H spectra to provide accurate integrals. Similarly, a 30 s recycle delay was used for all ^{31}P spectra.

The unoptimized isolated yield (68%) for the G4 PAMAM PIP_2 dendrimer **1** was determined by using ^{31}P NMR and trimethylphosphate as an internal standard. ^{1}H NMR (500 MHz, 80% D_2O) δ: 4.28−4.18 (m), 4.05−3.96 (m), 3.93−3.88 (qt), 3.74−3.73 (br s), 3.43 (br s), 3.30 (br s), 2.84 (br s), 2.79 (br s), 2.63 (br s), 2.45 (br s), 2.40 (br s), 1.98 (tr), 1.46 (m). ^{13}C NMR (DSS external reference) (125 MHz) δ: 182.1, 181.6, 175.1, 174.8, 169.0, 168.4, 77.1, 76.4, 75.1, 72.0, 70.9, 65.4, 63.5, 51.7, 51.6, 49.2, 44.0, 41.5, 40.3, 37.0, 32.8, 32.6, 31.7 (Supplementary Figure 3). ^{31}P NMR (202 MHz) δ: 5.43, 5.25, 0.48.

Acknowledgment: We thank A. Hansen and J. Karty for assistance with MALDI mass spectrometry. This work was partially funded by a Faculty Research Support Program award from the Office of the Vice Provost for Research at Indiana University, along with support from NSF grant MCB-9722264 and Indiana University. The U.S. Department of Education is thanked for support in the form of a GAANN fellowship to N.K.S. and S.M.R.

Supporting Information Available: This material is available free of charge *via* the Internet at http://pubs.acs.org.

REFERENCES

1. Cully, M., You, H., Levine, A. J., and Mak, T. W. (2006) Beyond PTEN mutations: the PI3K pathways as an integrator of multiple inputs during tumorigenesis, *Nat. Rev. Cancer 6*, 184–192.
2. Di Paolo, G., and De Camilli, P. (2006) Phosphoinositides in cell regulation and membrane dynamics, *Nature 443*, 651–657.
3. Niggli, V. (2001) Structural properties of lipid-binding sites in cytoskeletal proteins, *Trends Biochem. Sci. 26*, 604–611.
4. Janmey, P. A., and Lindberg, U. (2004) Cytoskeletal regulation: rich in lipids, *Nat. Rev. Mol. Cell Biol. 5*, 658–666.
5. De Matteis, M. A., and Godi, A. (2004) PI-loting membrane traffic, *Nat. Cell Biol. 6*, 487–492.
6. Haucke, V. (2005) Phosphoinositide regulation of clathrin-mediated endocytosis, *Biochem. Soc. Trans. 33*, 1285–1289.
7. Balla, T. (2005) Inositol-lipid binding motifs: signal integrators through protein−lipid and protein−protein interactions, *J. Cell Sci. 118*, 2093–2104.
8. Hurley, J. H. (2006) Membrane binding domains, *Biochem. Biophys. Acta 1761*, 805–811.
9. Lemmon, M. A. (2003) Phosphoinositide recognition domains, *Traffic 4*, 201–213.
10. Cho, W., and Stahelin, R. V. (2005) Membrane-protein interactions in cell signaling and membrane trafficking, *Annu. Rev. Biophys. Biomol. Struct. 34*, 119–151112 plates.
11. Lemmon, M. A. (2008) Membrane recognition by phospholipid-binding domains, *Nat. Rev. Mol. Cell Biol. 9*, 99–111.
12. Lassing, I., and Lindberg, U. (1985) Specific interaction between phsophatidylinositol 4,5-bisphosphate and profilactin, *Nature 314*, 835–838.
13. Goldschmidt-Clermont, P. J., Machesky, L. M., Baldassare, J. J., and Pollard, T. D. (1990) The actin-binding protein profilin binds to PIP_2 and inhibits its hydrolysis by phospholipase C, *Science 247*, 1575–1578.
14. Feng, L., Mejillano, M., Yin, H. L., Chen, J., and Prestwich, G. D. (2001) Full-contact domain labeling: Identification of a novel phosphoinositide binding site on gelsolin that requires the complete protein, *Biochemistry 40*, 904–913.
15. Wang, J., Gambhir, A., Hangyas-Mihalyne, G., Murray, D., Golbebiewska, U., and McLaughlin, S. (2002) Lateral sequesteration of phosphatidylinositol 4,5-bisphospate by the basic effector domain of myristolated alanine-rich C kinase substrate is due to nonspecific electrostatic interaction, *J. Biol. Chem. 277*, 34401–34412.
16. Yu, F. X., Sun, H. Q., Janmey, P., and Yin, H. L. (1992) Identification of a polyphosphoinositide binding sequence in an actin monomer-binding domain of gelsolin, *J. Biol. Chem. 267*, 14616–14621.
17. Lorenz, C. D., Faraudo, J., and Travesset, A. (2008) Hydrogen bonding and binding of polybasic residues with negatively charged mixed lipid monolayers, *Langmuir 24*, 1654–1658.

18. Carlton, J. G., and Cullen, P. J. (2005) Coincidence detection in phosphoinositide signaling, *Trends Cell Biol. 15*, 540–547.
19. Barret, C., Roy, C., Montcourrier, P., Mangeat, P., and Niggli, V. (2000) Mutagenesis of the phosphatidylinositol 4,5-bisphosphate (PIP_2) binding site in the NH_2-terminal domain of ezrin correlates with its altered cellular distribution, *J. Cell Biol. 151*, 1067–1080.
20. Bompard, G., Martin, M., Roy, C., Vignon, F., and Freiss, G. (2003) Membrane targeting of protein tyrosine phosphatase PTPL1 through its FERM domain *via* binding to phosphatidylinositol 4,5-biphosphate, *J. Cell Sci. 116*, 2519–2530.
21. Papayannopoulos, V., Co, C., Prehoda, K. E., Snapper, S., Taunton, J., and Lim, W. A. (2005) A polybasic motif allows N-WASP to act as a sensor of PIP_2 density, *Mol. Cell 17*, 181–191.
22. Berg, J. S., Derfler, B. H., Pennisi, C. M., Corey, D. P., and Cheney, R. E. (2000) Myosin-X, a novel myosin with pleckstrin homolgy domains, associates with regions of dynamic actin, *J. Cell Sci. 113*, 3439–3451.
23. Klein, D. E., Lee, A., Frank, D. W., Marks, M. S., and Lemmon, M. A. (1998) The pleckstrin homology domains of dynamin isoforms require oligomerization for high affinity phosphoinositide binding, *J. Biol. Chem. 273*, 27725–27733.
24. Mammen, M., Seok-Ki, C., and Whitesides, G. M. (1998) Polyvalent interactions in biological systems: implications for design and use of multivalent ligands and inhibitors, *Angew. Chem., Int. Ed. 37*, 2754–2794.
25. Kiessling, L. L., Gestwicki, J. E., and Strong, L. E. (2006) Synthetic multivalent ligands as probes of signal transduction, *Angew. Chem., Int. Ed. 45*, 2348–2368.
26. Lundquist, J. J., and Toone, E. J. (2002) The cluster glycosidic effect, *Chem. Rev. 102*, 555–578.
27. Wittenmayer, N., Jandrig, B., Rothkegel, M., Schlueter, K., Arnold, W., Haensch, W., Scherneck, S., and Jockusch, B. M. (2004) Tumor suppressor activity of profilin requires a functional actin binding site, *Mol. Biol. Cell 15*, 1600–1608.
28. Bae, Y. H., Ding, Z., Zou, L., Wells, A., Gertler, F., and Roy, P. (2009) Loss of profilin-1 expression enhances breast cancer cell motility by Ena/VASP proteins, *J. Cell. Physiol. 219*, 354–364.
29. Das, T., Bae, Y. H., Wells, A., and Roy, P. (2008) Profilin-1 overexpression upregulates PTEN and suppresses AKT activation in breast cancer cells, *J. Cell. Physiol. 218*, 436–443.
30. Witke, W. (2004) The role of profilin complexes in cell motility and other cellular processes, *Trends Cell Biol. 14*, 461–469.
31. Jockusch, B. M., Murk, K., and Rothkegel, M. (2007) The profile of profilins, *Rev. Physiol., Biochem., Pharmacol. 159*, 131–149.
32. Lu, P. J., Shieh, W. R., Rhee, S. G., Yin, H. L., and Chen, C. S. (1996) Lipid products of phosphoinositide 3-kinase bind human profilin with high affinity, *Biochemistry 35*, 14027–14033.
33. Machesky, L. M., Goldschmidt-Clermont, P. J., and Pollard, T. D. (1990) The affinities of human platelet and Acanthamoeba profilin isoforms for polyphosphoinositides account for their relative abilities to inhibit phospholipase C, *Cell Reg. 1*, 937–950.
34. Lambrechts, A., Jonckheere, V., Dewitte, D., Vandekerckhove, J., and Ampe, C. (2002) Mutational analysis of human profilin I reveals a second PI(4,5)-P_2 binding site neighbouring the poly(L-proline) binding site, *BMC Biochem. 3*, 12.
35. Sathish, K., Padma, B., Munugalavadla, V., Bhargavi, V., Radhika, K. V. N., Wasia, R., Sairam, M., and Singh, S. S. (2004) Phosphorylation of profilin regulates its interaction with actin and poly (L-proline), *Cell Signalling 16*, 589–596.
36. Sohn, R. H., Chen, J., Koblan, K. S., Bray, P. F., and Goldschmidt-Clermont, P. J. (1995) Localization of a binding site for phosphatidylinositol 4,5-bisphosphate on human profilin, *J. Biol. Chem. 270*, 21114–21120.
37. Goldschmidt-Clermont, P. J., Kim, J. W., Machesky, L. M., Rhee, S. G., and Pollard, T. D. (1991) Regulation of phospholipase C-γ1 by profilin and tyrosine phosphorylation, *Science 251*, 1231–1233.
38. Tomalia, D. A., Naylor, A. M., and Goddard Iii, W. A. (1990) Starburst dendrimers: molecular-level control of size, shape, surface chemistry, topology, and flexibility from atoms to macroscopic matter, *Angew. Chem., Int. Ed. Engl. 29*, 138–175.
39. Naylor, A. M., Goddard Iii, W. A., Kiefer, G. E., and Tomalia, D. A. (1989) Starburst dendrimers. 5. Molecular shape control, *J. Am. Chem. Soc. 111*, 2339–2341.
40. Prestwich, G. D. (1996) Touching all the bases: synthesis of inositol polyphosphate and phosphoinositide affinity probes from glucose, *Acc. Chem. Res. 29*, 503–513.
41. Prestwich, G. D., Marecek, J. F., Mourey, R. J., Theibert, A. B., Ferris, C. D., Danoff, S. K., and Snyder, S. H. (1991) Tethered IP_3. Synthesis and biochemical applications of the 1-*O*-(3-aminopropyl) ester of inositol 1,4,5-triphosphate, *J. Am. Chem. Soc. 113*, 1822–1825.
42. Gou, D. M., Liu, Y. C., and Chen, C. S. (1992) An efficient chemoenzymic access to optically active myo-inositol polyphophates, *Carbohydr. Res. 234*, 51–64.
43. Webb, S. A., Stewart, N. K., Belcher, L. J., Mechref, Y., Tomaszewski, J. W., Wu, G., Novotny, M. V., and Oakley, M. G. (2007) Synthesis and characterization of covalent mimics of phosphatidylinositol-4,5-bisphosphate micelles, *Biomacromolecules 8*, 1790–1793.
44. Sugiura, Y. (1981) Structure of molecular aggregates of 1-(3-*sn*-phosphatidy)-L-myo-inositol 3,4-bis(phosphate) in water, *Biochim. Biophys. Acta 641*, 148–159.
45. Tolic, L. P., Anderson, G. A., Smith, R. D., Brothers Ii, H. M., Spindler, R., and Tomalia, D. A. (1997) Electrospray ionization Fourier transform ion cyclotron resonance mass spectrometric characterization of high molecular mass Starburst dendrimers, *Int. J. Mass Spectrom. Ion Processes 165/166*, 405–418.
46. Woller, E. K., and Cloninger, M. J. (2001) Mannose functionalization of a sixth generation dendrimer, *Biomacromolecules 2*, 1052–1054.
47. Woller, E. K., and Cloninger, M. J. (2002) The lectin-binding properties of six generations of mannose-functionalized dendrimers, *Org. Lett. 4*, 7–10.
48. Tietze, L. F., Arlt, M., Beller, M., Glusenkamp, K., Jahde, E., and Rajewsky, M. F. (1991) Squaric acid diethyl ester: A new coupling reagent for the formation of drug biopolymer conjugates. Synthesis of squaric acid ester amides and diamides, *Chem. Ber. 124*, 1215–1221.
49. Wittenmayer, N., Rothkegel, M., Jockusch, B. M., and Schluter, K. (2000) Functional characterization of green fluorescent protein-profilin fusion proteins, *Eur. J. Biochem. 267*, 5256.
50. Bjorkegren-Sjogren, C., Korenbaum, E., Nordberg, P., Lindberg, U., and Karlsson, R. (1997) Isolation and characterization of two mutants of human profilin I that do not bind poly(L-proline), *FEBS Lett. 418*, 258–264.
51. Chaudhary, A., Chen, J., Gu, Q.-M., Witke, W., Kwiatkowski, D. J., and Prestwich, G. D. (1998) Probing the phosphoinositide 4,5-bisphosphate binding site of human profilin I, *Chem. Biol. 5*, 273–281.
52. Lassing, I., and Lindberg, U. (1988) Specificity of the interaction between phosphatidylinositol 4,5-bisphosphate and the profilin:actin complex, *J. Cell. Biochem. 37*, 255–267.
53. Richer, S. M., Stewart, N. K., Tomaszewski, J. W., Stone, M. J., and Oakley, M. G. (2008) NMR investigation of the binding between human profilin I and inositol 1,4,5-triphosphate, the soluble headgroup of phosphatidylinositol 4,5-bisphosphate, *Biochemistry 47*, 13455–13462.
54. Moens, P. D. J., and Bagatolli, L. A. (2007) Profilin binding to sub-micellar concentrations of phosphatidylinositol (4,5) bisphosphate and phosphatidylinositol (3,4,5) trisphosphate, *Biochim. Biophys. Acta, Biomembr. 1768*, 439–449.
55. DiNitto, J. P., and Lambright, D. G. (2006) Membrane and juxtamembrane targeting by PH and PTB domains, *Biochim. Biophys. Acta, Mol. Cell Biol. Lipids 1761*, 850–867.
56. Prestwich, G. D. (2004) Phosphoinositide signaling: From affinity probes to pharmaceutical targets, *Chem. Biol. 11*, 619–637.
57. Ferguson, C. G., James, R. D., Bigman, C. S., Shepard, D. A., Abdiche, Y., Katsamba, P. S., Myszka, D. G., and Prestwich, G. D. (2005) Phosphoinositide-containing polymerized liposomes: stable membrane-mimetic vesicles for protein-lipid binding analysis, *Bioconjugate Chem. 16*, 1475–1483.
58. Gong, D., Smith, M. D., Manna, D., Bostic, H. E., Cho, W., and Best, M. D. (2009) Microplate-based characterization of protein-phosphoinositide binding interactions using a synthetic biotinylated headgroup analogue, *Bioconjugate Chem. 20*, 310–316.
59. Wang, D. S., and Chen, C. S. (1996) Synthesis of the D-3 series of phosphatidylinositol phosphates, *J. Org. Chem. 61*, 5905–5910.
60. Janmey, P. A., Iida, K., Yin, H. L., and Stossel, T. P. (1987) Polyphosphoinositide micelles and polyphosphoinositide-containing vesicles dissociate endogenous gelsolin-actin complexes and promote actin assembly from the fast-growing end of actin filaments blocked by gelsolin, *J. Biol. Chem. 262*, 12228–12236.
61. Narayan, K., and Lemmon, M. A. (2006) Determining selectivity of phosphoinositide-binding domains, *Methods (San Diego, CA, U.S.) 39*, 122–133.

62. Woller, E. K., Walter, E. D., Morgan, J. R., Singel, D. J., and Cloninger, M. J. (2003) Altering the strength of lectin binding interactions and controlling the amount of lectin clustering using mannose/hydroxyl-functionalized dendrimers, *J. Am. Chem. Soc. 125*, 8820–8826.
63. Wolfenden, M. L., and Cloninger, M. J. (2005) Mannose/glucose-functionalized dendrimers to investigate the predictable tunability of multivalent interactions, *J. Am. Chem. Soc. 127*, 12168–12169.
64. Wolfenden, M. L., and Cloninger, M. J. (2006) Carbohydrate-functionalized dendrimers to investigate the predictable tunability of multivalent interactions, *Bioconjugate Chem. 17*, 958–966.
65. Fedorov, A. A., Pollard, T. D., and Almo, S. C. (1994) Purification, characterization and crystallization of human platelet profilin expressed in *Escherichia coli*, *J. Mol. Biol. 241*, 480–482.
66. Furutani, M., Tsujita, K., Itoh, T., Ijuin, T., and Takenawa, T. (2006) Application of phosphoinositide-binding domains for the detection and quantification of specific phosphoinositides, *Anal. Biochem. 355*, 8–18.
67. Huff, S., Matsuka, Y. V., McGavin, M. J., and Ingham, K. C. (1994) Interaction of N-terminal fragments of fibronectin with synthetic and recombinant D motifs from its binding protein on *Staphylococcus aureus* studied using fluorescence anisotropy, *J. Biol. Chem. 269*, 15563–15570.
68. Ye, J., Kohli, L. L., and Stone, M. J. (2000) Characterization of binding between the chemokine eotaxin and peptides derived from the chemokine receptor CCR3, *J. Biol. Chem. 275*, 27250–27257.
69. Laue, T. M., Shah, B., Ridgeway, T. M., and Pelletier, S. L. (1992) Computer-aided interpretation of analytical sedimentation data for proteins, *Anal. Ultracentrifugation Biochem. Polym. Sci.* 90–125.
70. Nourse, A., Millar, D. B., and Minton, A. P. (2000) Physicochemical characterization of generation 5 polyamidoamine dendrimers, *Biopolymers 53*, 316–328.
71. Chen, J., Feng, L., and Prestwich, G. D. (1998) Asymmetric total synthesis of phosphatidylinositol 3-phosphate and 4-phosphate derivatives, *J. Org. Chem. 63*, 6511–6522.
72. Humphrey, W., Dalke, A., and Schulten, K. (1996) VMD- visual molecular dynamics, *J. Mol. Graphics 14.1*, 33–38.